JOURNAL OF MATERIALS SCIENCE 21 (1986) 2059–2066

# The preyield evolution with strain of the work-hardening rate in glassy polymers (PABM resin)

G. COULON, J. M. LEFEBVRE, B. ESCAIG
*Laboratoire de Structure et Propriétés de l'Etat Solide, CNRS (LA 234) Université des Sciences et Techniques de Lille, 59655 Villeneuve d'Ascq Cedex, France*

The work-hardening rate $K$, measured in the early preyield stage of constant strain-rate compression tests, is found to vary as the inverse of the non-elastic strain $\varepsilon_p$. From a metallurgical point of view, we show that, in the early stage of development of thermally activated glide processes, this behaviour can be predicted from simple assumptions on the shear nuclei kinetics. The $\varepsilon_p$-dependence of $K$ is tested in the case of a tightly cross-linked polyimide polyamino-bismaleimide, PABM, resin.

## 1. Introduction

In previous papers [1–3] we have shown that the work-hardening rate $K$, measured in the preyield stage, is a very sensitive probe of any microstructural evolution and of its influence on the non-elastic behaviour of glassy polymers. From a metallurgical point of view [4], as the non-elastic strain $\varepsilon_p$ increases in the preyield stage, an internal stress field $\sigma_i$ grows up from nucleated defects and the parameter $K$ can be defined as:

$$K = \frac{d\sigma_i}{d\varepsilon_p} = \left(\frac{\partial\sigma}{\partial\varepsilon_p}\right)_{\dot{\varepsilon},T} \quad (1)$$

where stress value, $\sigma = \sigma_i(\varepsilon_p) + \sigma^*(T, \dot{\varepsilon}_p)$ is the flow stress corresponding to the total strain $\varepsilon_t = \varepsilon_H + \varepsilon_p$, where $\varepsilon_H$ is the Hookean elastic part of the strain.

Recent neutron experiments [5] on deformed glassy polymers have emphasized that deformation processes in the solid glassy phase are quite localized events: distortions in bonding have to be strictly confined within cores of defects in the molecular arrangement (much like dislocation lines of the Somigliana type), the propagation of which produces a local shear strain. It is well known that the deformation zones appear clearly below the conventional yield stress [6], so that the critical shear nuclei (or defects) which are the precursors of the non-elastic macroscopic strain should nucleate and expand in the preyield stage. The closer the applied stress gets to the yield stress, the more profuse the shearing is, leading to a flow of the solid at yield. The physical meaning of shear defects has been already given in a previous paper [7].

The property of nucleating defects, i.e. the ability of a given polymer to deform non-elastically, should be related to its microstructure: as an example, it has been found clearly dependent upon the degree of cross-linking of a polyimide resin [2, 8] (i.e. to its initial microstructure). In previous papers [1–3] we propose to relate the parameter $K$ to the defect nucleation rate by making the simplifying assumption that, in the preyield stage, the sole defect nucleation is responsible for the non-elastic strain $\varepsilon_p$ so that:

$$K \sim (\partial N/\partial\sigma)^{-1}_{\dot{\varepsilon},T} \quad (2)$$

where $(\delta N/\partial\sigma)$ is the net number of defects produced by unit stress.

In the specific case of thermoset polyimide resins [2, 8] $K$ measurements proved to be very efficient to follow the evolution of cross-linking with curing time. Whereas usual macroscopic mechanical quantities such as the Young's modulus $M$ or the yield stress $\sigma_y$ did not vary noticeably with curing time, in contrast, the parameter $K$, measured at a constant non-elastic strain $\varepsilon_p = 4 \times 10^{-3}$, increased uniformly by almost a factor of three between the minimum curing (3 h at 200°C) and the most complete one (24 h at 200°C plus 24 h at 250°C).

Such results led us to propose that the longer the curing time of a PABM polyimide resin, the harder the nucleation of plasticity defects and thus the poorer the ability of the resin to deform plastically.

The purpose of this paper is to make a further step in our metallurgical approach of the non-elastic behaviour of glassy polymers. As shown in the next section it can be predicted from simple assumptions that, in the early stage of development of thermally activated glide processes, the $K$ parameter is expected to vary as $(\varepsilon_p)^{-1}$, as an example in the preyield stage of a constant strain-rate test. We have chosen to test this prediction in the case of a PABM resin cured for 24 h at 200°C as from recent thermodynamical analysis [9] the mechanical behaviour of this tightly cross-linked resin over the whole temperature range exhibits only one deformation mode: the so-called activated glide mode characterized by a stress dependent activation energy and by a strong and homogeneous birefringence in the shear band. Coherent neutron scattering experiments have shown that the simple shear geometry clearly visible on external surfaces is

0022–2461/86 $03.00 + .12 

unchanged at any scale down to about 1.5 nm [10, 11]. The measurement of $K$ and its experimental $\varepsilon_p$-dependence are reported in Section 3 while the last section is devoted to discussion.

## 2. The defect kinetics model in the preyield stage of a glide process

The work-hardening rate $K$ is a function of both the non-elastic strain $\varepsilon_p$ and the microstructure. We intend to follow here, for a given microstructure, the experimental variation of $K$ along the preyield stage of a constant strain-rate test, and see how this variation can be explained in terms of plasticity defects. More specifically, we consider the case of a glide deformation mode [4].

In the early beginning of preyield stage, the deformation mechanism is primarily governed by defect nucleation. At a given stress value $\sigma$, which means a given time $t$ in a constant strain-rate test, number $N$ of defects have been both nucleated and propagated. As long as $\sigma$ is far below the yield, the motion of mobile defects through the amorphous bulk, once they have been nucleated, should be rather limited in extension. As a result, the cumulative non-elastic strain $\varepsilon_p$ built up in the material at time $t$ may be modelled only in terms of nucleation steps. Furthermore, since any annihilation, overlap or interaction of defects may be tentitatively neglected, $\varepsilon_{p_0}$ can be viewed as the average "free" strain each one of the $N$ shear nuclei contributes to $\varepsilon_p$ after it has achieved "full" expansion as if it were isolated:

$$\varepsilon_p = N\varepsilon_{p_0} \tag{3}$$

Along the same line, but taking $\varepsilon_{p_0}$ as stress independent, the non-elastic strain $d\varepsilon_p$ produced by the applied stress increment $d\sigma$ is:

$$d\varepsilon_p = \varepsilon_{p_0} dN \tag{4}$$

The above nucleation scheme can be complemented by a nucleation law for defect multiplication, which is usually chosen to be exponential. Consistently with the above assumptions (no annihilation processes), increasing the applied stress by $d\sigma$ should create a number $dN$ of defects:

$$dN \sim N d\sigma \tag{5}$$

where $N$ is the number of defects already created at a stress value $\sigma$, for a given strain-rate $\dot{\varepsilon}$. This leads to the nucleation law:

$$N = N_0 \exp B\sigma \tag{6}$$

in which $N_0$ is the zero stress, pre-existing defect number in the material and $B$, the stress independent nucleation constant which we relate in the following to the stress sensitivity of strain-rate in the preyield stage.

Within this very simple framework, the work-hardening rate $K$ can be viewed as a measure of the defect nucleation rate since, following Equations 1, 3, 4 and 6, one has:

$$K = \frac{d\sigma_i}{d\varepsilon_p} = \left(\frac{\partial\sigma}{\partial\varepsilon_p}\right)_{\dot{\varepsilon},T} = \frac{1}{\varepsilon_{p_0}}\left(\frac{\partial N}{\partial\sigma}\right)^{-1}_{\dot{\varepsilon},T} \tag{7}$$

or

$$K = \frac{1}{B\varepsilon_p} \tag{8}$$

Therefore $K$ should vary as the inverse of the non-elastic strain $\varepsilon_p$ along the early part of the preyield stage.

In order to test this prediction and precisely to state its validity range, the factor $B$ has first to be related to available experimental quantities, and measured. This is done in probing the stress sensitivity of the strain kinetics valid in the early part of the preyield stage, as we now demonstrate.

As time progresses during a constant strain-rate test, the increase in non-elastic strain with time is derived from two distinct processes. First, time is allowed for further activating the propagation of the $N$ defects already existing at time $t$. The activation rate $R$ has the usual Arrhenius form for activated processes [4]:

$$R = \nu_N \exp(-\Delta G_a/kT) \tag{9}$$

where $\nu_N$ is the attempt frequency of a given defect for overcoming the cage potential well made by neighbouring molecular segments, and the exponential is the Boltzmann chance of success of an energy fluctuation of strength $\Delta G_a$, the activation energy. Second, the stress increases during time, which leads both to the nucleation law given in Equation 6, and to an increase in the activation rate $R$ since $\Delta G_a$ is a decreasing function of the variable $\sigma - \sigma_i$. The resulting strain-rate is simply evaluated as usual [4, 12]:

$$\dot{\varepsilon}_p = N\varepsilon_{p_0} R \tag{10}$$

where $\varepsilon_{p_0}$ is the average one defect-strain produced either by a successful nucleation or propagation event, as introduced above. This is because the defect expansion occurring during nucleation is likely to have the same range as the one occurring during propagation of an already existing defect, for the latter can be described geometrically as the nucleation of a localized extra defect loop attached to the main defect, and because such expansions should be limited mainly by the local molecular structure of the amorphous material itself [13].

Equation 10 can be easily established. Let us assume the non-elastic strain at time $t$ is $\varepsilon_p$; at time $t + dt$ it becomes $\varepsilon_p + d\varepsilon_p$, where $d\varepsilon_p$ is the sum of the two preceding contributions, that is:

$$d\varepsilon_p = \varepsilon_{p_0}(NR\,dt) + (\varepsilon_{p_0} dt)\,[d(NR)/d\sigma]\,d\sigma \tag{11}$$

or

$$\dot{\varepsilon}_p = \varepsilon_{p_0} NR + \varepsilon_{p_0}\dot{\sigma}[d(NR)/d\sigma]\,dt \tag{12}$$

with $\dot{\sigma} = d\sigma/dt$; this quantity remains finite when $dt \to 0$, since $\dot{\sigma} = K\dot{\varepsilon}_p$; as does $d(NR)/d\sigma = NR[B + (V_a/KT)]$, where $V_a = -d(\Delta G_a)/d\sigma$. Equation 10 follows then at the limit $dt \to 0$.

Equations 9 and 10 together with Equation 6 give the non-elastic strain-rate in the preyield stage as:

$$\dot{\varepsilon}_p = N_0\varepsilon_{p_0}\nu_N \exp\left(\frac{V_n\sigma}{kT}\right)\exp\left[-\frac{\Delta G_a(\sigma - \sigma_i)}{kT}\right] \tag{13}$$

where for convenience, the nucleation constant $B$ has been taken as

$$B = V_n/kT \quad (14)$$

Here the nucleation parameter, $V_n$, has the dimension of a volume but has otherwise no particular physical meaning, since *no thermal activation* is assumed to occur in nucleation events; $\sigma_i$ is the internal stress field originating from defects and $\sigma - \sigma_i$ is termed the effective stress.

Equation 13 looks like the usual Ree–Eyring equation but differs from it in as much as: (i) the pre-exponential factor has been expanded in terms of nucleation parameters and (ii) the activation energy is not assumed to be a linear function of stress. In reality, its stress derivative at yield, $V_a = -(\partial \Delta G_a/\partial \sigma)$, has been measured (see Fig. 5 below); it is seen that $V_a$ is not a constant as assumed in the Ree–Erying theory, but increases with increasing the yield stress, i.e. decreasing the temperature, as it is exemplified quite extensively in low temperature crystalline plasticity.

Equation 13 allows us to identify the parameter $V_n$. In a stress-relaxation test [4, 14], the available experimental quantity is the "apparent" activation volume defined as:

$$V_0 = kT\left(\frac{\partial \ln \dot{\varepsilon}_p}{\partial \sigma}\right)_{T,\sigma_i} \quad (15)$$

Assuming $N_0 \varepsilon_{p_0} v_N$ in Equation 13 does not depend on stress, this equation leads to:

$$V_0 = V_n - \left(\frac{\partial \Delta G_a(\sigma - \sigma_i)}{\partial \sigma}\right)_{T,\sigma_i} = V_n + V_a \quad (16)$$

where $V_a$, the "true" activation volume, is identified from the Second Law of Thermodynamics as the opposite of the stress derivative of $\Delta G_a$.

This last equation shows us the apparent activation volume in the preyield stage is made of a nucleation parameter, $V_n$, and a propagation parameter $V_a$. The latter can be measured from the apparent volume observed at yield, at the temperature $T'$ where the yield stress is equal to the stress at which $V_0$ is measured, $\sigma_y(T') = \sigma$, so that $V_a(\sigma, T) = V_0(\sigma_y, T')$. This is because at yield, a steady state defect number is set up within the material due to a balance between nucleation and annihilation processes, so that $N$ becomes constant in Equation 10 and only the propagation term $R$ prevails in the stress sensitivity of $\dot{\varepsilon}_p$, implying $V_a(\sigma_y, T') = V_0(\sigma_y, T')$ instead of Equation 16. Now, since $V_a$ can be reasonably assumed to depend only on stress [4], together with $\sigma_y(T') = \sigma$, it comes $V_a(\sigma) = V_a(\sigma_y, T') = V_0(\sigma_y = \sigma, T')$. Hence:

$$V_n = V_0(\sigma, T) - V_0(\sigma_y = \sigma, T') \quad (17)$$

or

$$K = \left(\frac{kT}{V_0(\sigma, T) - V_0(\sigma_y = \sigma, T')}\right)\left(\frac{1}{\varepsilon_p}\right) \quad (18)$$

## 3. Experimental procedure

### 3.1. Preparation and curing of PABM polyimide samples

Polyamino-bismaleimide (PABM) samples were provided by Rhône Poulenc Industries. These were prepared by reaction at 180° C of 2.5 mol 4,4′-diphenylmethane bismalemide:

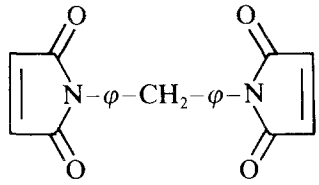


with 1 mol diamino 4,4′-diphenylmethane: $H_2N-\varphi-CH_2-\varphi-NH_2$. Both homopolymerization and polyaddition with diamine occur during reaction and curing; this results in a cross-linked thermoset resin, the glass transition temperature of which is over 300° C.

Parallelepipedic PABM resin plates 120 mm × 70 mm × 12 mm are then cured for 24 h at 200° C in air. A previous study [1, 8] has shown that this thermal treatment leads to a tighted cross-linked resin. Compression samples were then cut from the sheets and machine turned into small cylindrical specimens (6 mm diameter and 11 mm long); they were mechanically polished carefully to ensure that end sections were parallel to better than 0.01 mm.

### 3.2. Mechanical tests

Two series of tests have been performed with the purpose of:

(i) measuring directly the $\varepsilon_p$-dependence of the work-hardening rate $K$ at room temperature along the preyield stage;

(ii) measuring the apparent activation volume $V_0$ at yield for different temperatures, i.e. the term $V_a(\sigma, T)$, in order to evaluate the parameter $V_n$ independently from (i).

#### *3.2.1. Measurement of $K(\varepsilon_p)$*

The method of measuring $K$ has been already given in detail in previous papers [1, 2, 4], so we mention here only the main features.

During compression tests at constant total strain rate $\dot{\varepsilon}_t$ and constant temperature $K$ is measured by stress relaxation from some stress valeur $\sigma_0$ i.e. at some non-elastic strain $\varepsilon_p$. In the present experiments, the degree of cross-linking of the PABM resin does not vary and $K$ is only a function of $\varepsilon_p$. The evaluation of $K$ at a given $\varepsilon_p$ needs two samples be tested at this $\varepsilon_p$ value: a single relaxation test which leads to the value of the experimental activation volume $V_{exp}$ and 8 to 10 successive relaxation tests which yield the quantity $(V_0 K/M)$ where $M$ is Young's modulus and $V_0$ the apparent activation volume defined in Equation 16.

Let us recall that during the relaxation test the observed stress evolution with time is:

$$\Delta\sigma(t) = -(kT/V_{exp}) \log [1 + (t/c)] \quad (19)$$

with $V_{exp} = V_0 + (V_0 K/M)$, and time constant $c$ [1, 2, 4]. The corrective term $(V_0 K/M)$ is due to work-hardening by the defects nucleated during the relaxation test itself; in the preyield stage, it is usually larger than $V_0$.

During the successive relaxation test the observed duration of the $n$th relaxation increases exponentially

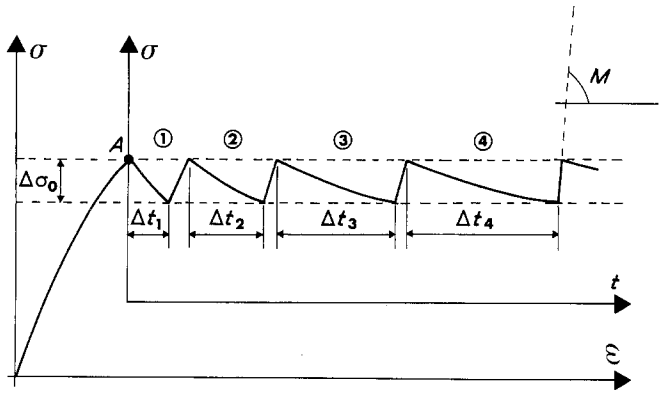


*Figure 1* The successive stress relaxation test.

with the number $n$ [15] as:

$$\Delta t_n = \Delta t_1 \exp [(n - 1)KV_0\Delta\sigma_0/kT] \quad (20)$$

as soon as $n$ is larger than a few units and provided that $\Delta\sigma_0$ be chosen small enough, $V_0\Delta\sigma_0 < kT$ (Fig. 1).

By measuring $M$ at the beginning of the stress–strain curve the value of $K$ at a given $\varepsilon_p$ can be determined from Equations 19 and 20 while the corresponding $\varepsilon_p$ value is known from the equation: $\varepsilon_p = \varepsilon_t - (\sigma/M)$ where the total strain $\varepsilon_t$ is measured by an LVDT transducer rigidly attached to the fixed compression plate with its tip at the mobile plate [9].

The results presented in the following have been obtained for compression tests performed with an Instron machine at constant strain-rate $\dot{\varepsilon}_t = 3 \times 10^{-5}\,\text{sec}^{-1}$ and at room temperature, $T = 293\,\text{K}$. In one relaxation test, typical conditions are of 5 min duration, a corresponding stress drop $\Delta\sigma$ varying from 1.8 MPa ($\sigma = 110\,\text{MPa}$) to 8.8 MPa ($\sigma = 200\,\text{MPa}$) and time constant $c = 70$ to 80 sec. Successive relaxation tests have been performed with a constant stress drop $\Delta\sigma_0 \simeq 0.53\,\text{MPa}$.

The evolution of $V_{exp}$ and $(V_0K/M)$ with $\varepsilon_p$ are shown in Figure 2. The investigated $\varepsilon_p$ range runs from $2 \times 10^{-3}$ to $25 \times 10^{-3}$, but it must be noticed that only the measurements performed within the range $5 \times 10^{-3} < \varepsilon_p < 15 \times 10^{-3}$ are reliable. For, at smaller $\varepsilon_p$ values, measured values of $V_{exp}$ are quite inaccurate because of the great sensitivity of $V_{exp}$ with $\varepsilon_p$; at higher $\varepsilon_p$ values, measurements of $K$ are difficult, because, at the end of the preyield stage, $\varepsilon_p$ varies so quickly that it is very hard to stop the machine at the chosen $\varepsilon_p$; in addition, $K$ decreases to very small values and the duration of successive relaxations, $\Delta t_n$ in Equation 20, does not vary enough to permit any accurate determination of $K$.

Fig. 3 shows the variation of $\log_{10}(K/M)$ with $\log_{10}\varepsilon_p$. The $(K/M)$ values have been obtained from the measured values of $V_{exp}$ and $(V_0K/M)$ according to the relation:

$$K/M = \frac{V_0K/M}{V_{exp} - (V_0K/M)} \quad (21)$$

It can be seen that over the reliable $\varepsilon_p$-range the experimental points tend to be aligned, the slope of the

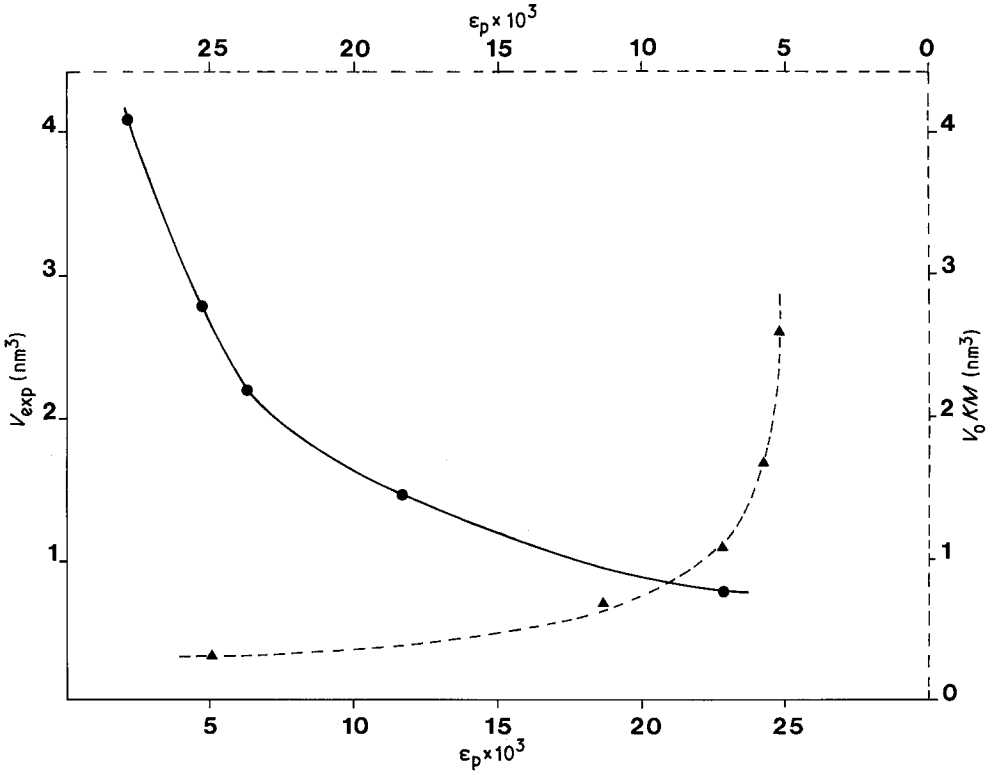


*Figure 2* The experimental activation volume $V_{exp}$ and the corrective term $V_0K/M$ versus the non-elastic strain $\varepsilon_p$; $M = 3890\,\text{MPa}$.

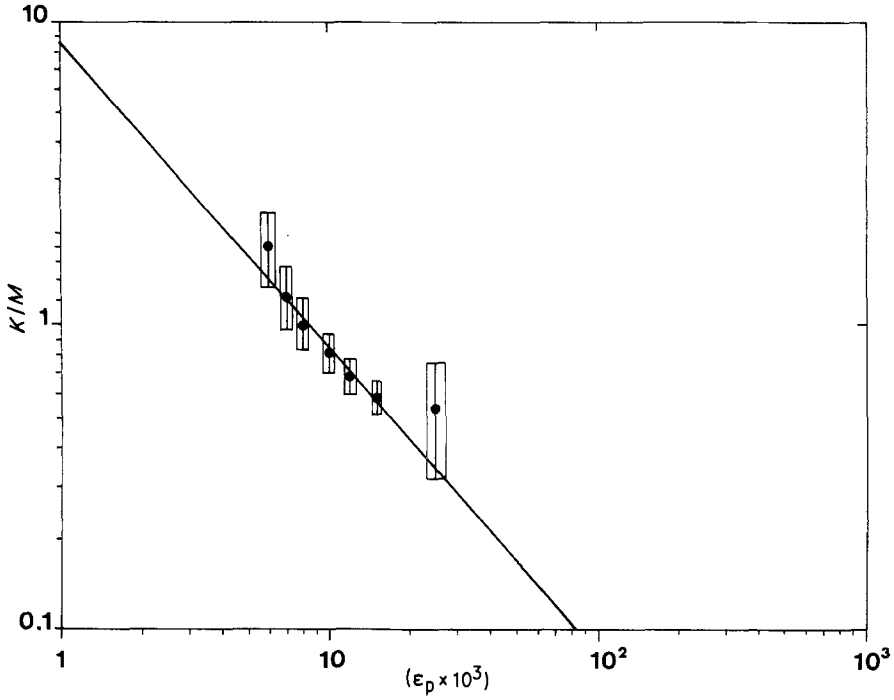


*Figure 3* The experimental variation of $K/M$ with $\varepsilon_p$: $\log_{10}(K/M)$ is plotted versus $\log_{10}\varepsilon_p$.

straight line being equal to $(-1 \pm 1\%)$. It follows that $(K/M)$ can be written as: $(K/M) = \alpha/\varepsilon_p$; the parameter $\alpha$ is easily deduced from the intersection of the straight line with the $\varepsilon_p$ axis: $\alpha = 8 \times 10^{-3}$. According to Equation 14, $\alpha$ can be expressed in terms of $V_n$: $\alpha = kT/MV_n$; knowing the experimental value of Young's modulus $M = 3890$ MPa, the value of $V_n$ reads thus: $V_n = 0.13\,\text{nm}^3$.

### 3.2.2. Measurement of the activation volume $V_a(\sigma_y, T)$ at yield at different temperatures

This experiment will be described more completely in a forthcoming paper [9].

Let us recall briefly the experimental conditions: compression tests have been performed with an Instron machine at constant total strain rate $\dot{\varepsilon}_t = 3 \times 10^{-5}\,\text{sec}^{-1}$ in a temperature range from 190 to 473 K. At each given temperature a relaxation test has been performed at yield during 5 min, the time constant $c$ varying from 90 to 120 sec with decreasing temperature.

Figs 4 and 5 show the observed variation with temperature of the yield stress $\sigma_y$ and of the experimental activation volume $V_{exp}$ respectively.

As recalled above, at yield $K = 0$ so that the corrective term in $V_{exp}$, $V_0K/M$, is negligible; therefore $V_{exp}(\sigma_y, T) = V_0(\sigma_y, T)$. Furthermore, in the case of

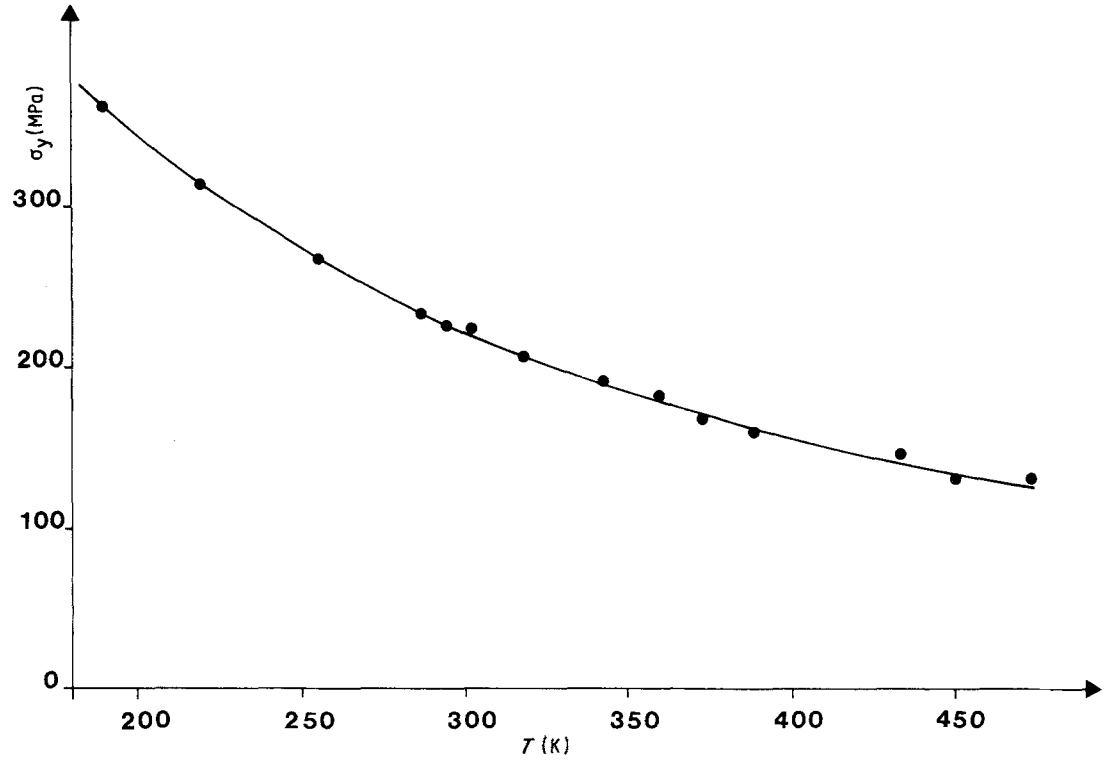


*Figure 4* The temperature-dependence of the yield stress $\sigma_y$ measured in a constant strain-rate compression test ($\dot{\varepsilon}_t = 3 \times 10^{-5}\,\text{sec}^{-1}$).

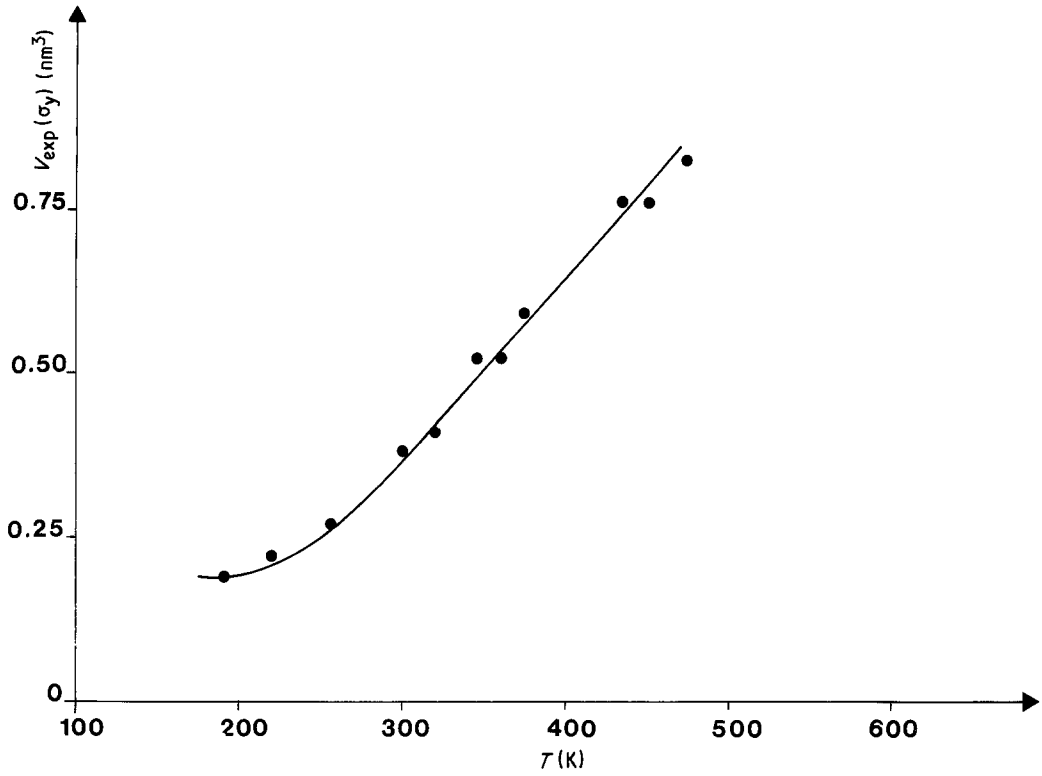


*Figure 5* The temperature-dependence of the experimental activation volume $V_{exp}$ measured at yield.

a thermally activated glide mode, the plastic flow at yield can be written: $\dot{\varepsilon}_p = \dot{\varepsilon}_0 \exp[\Delta G_a(\sigma - \sigma_i)/kT]$ where $\dot{\varepsilon}_0$ is negligibly stress dependent, hence $V_0(\sigma_y, T) = V_a(\sigma_y, T)$. Finally, Fig. 5 shows the temperature dependence of the "true" activation volume $V_a(\sigma_y, T)$ at yield.

It is now possible to calculate $V_n$ from Equation 17. We calculate it at two $\varepsilon_p$ values, chosen near the ends of the range where the linear behaviour of $\log_{10}(K/M)$ against $\log_{10}\varepsilon_p$ is observed, $\varepsilon_{p_{min}} = 7 \times 10^{-3}$ (or $\sigma = 135$ MPa) and $\varepsilon_{p_{max}} = 15 \times 10^{-3}$ (or $\sigma = 170$ MPa). On one hand, corresponding values of $V_0$ are deduced from Fig. 2 ($V_0 = V_{exp} - (V_0 K/M)$), $V_0(\varepsilon_{p_{min}}) = 0.90\,nm^3$ and $V_0(\varepsilon_{p_{max}}) = 0.72\,nm^3$. On the other hand, the relevant values of $V_0(\sigma_y = \sigma, T') = V_{exp}(\sigma_y, T') = V_a(\sigma)$ are obtained from Fig. 6, $V_a(\sigma = 135\,MPa) = 0.77\,nm^3$ and $V_a(\sigma = 170\,MPa) = 0.57\,nm^3$. Finally, the values of $V_n$ are evaluated: at $\varepsilon_{p_{min}} = 7 \times 10^{-3}$, $V_n = 0.13\,nm^3$, at $\varepsilon_{p_{max}} = 15 \times 10^{-3}$, $V_n = 0.15\,nm^3$.

It is noteworthy to see how these values are in good accordance with the one found in the direct measurement of $K(\varepsilon_p)$. The slight observed difference can be easily assigned to the precision of measurements, thus giving a full experimental check of Equation 18.

## 4. Discussion

The above results give some light upon the nucleation of shear defects, a major process still poorly known in the metallurgical approach of mechanical properties of thermoset polymeric resins. They rely on two main assumptions: (i) no defect annihilation nor interaction (limited defect extension), i.e. they belong to the early part of preyield stage, and (ii) no thermal activation of nucleation processes, nor any recovery phenomena, i.e. they belong to the lower temperature range of polymer plasticity (deformation in the glide mode). This last assumption resembles the usual situation in crystalline plasticity where Franck–Read mills cannot be helped by thermal agitation, due to too large a number of atoms to be activated for a dislocation loop to overcome critical configurations. Under these conditions the nucleation constant $B$ in Equation 6 is measured for our PABM resin by the value: $B = (V_n/kT) = 3.5 \times 10^{-8}\,Pa^{-1}$, corresponding to an average value $V_n = 0.14\,nm$ and $T = 293\,K$; or equivalently, putting $B = \sigma_B^{-1}$, one measures: $\sigma_B = 29\,MPa$. This means that, at the stress level of the present experiment ($\sim 150\,MPa$) the number of defects increases clearly exponentially with stress. Furthermore, from Equations 1 and 8, $d\sigma_i = \sigma_B d\varepsilon_p/\varepsilon_p$, so that the mean internal stress field originating from shear defects rises up logarithmically with non elastic strain while deforming at a constant strain-rate:

$$\sigma_i(\varepsilon_{p2}) - \sigma_i(\varepsilon_{p1}) = \sigma_B \log(\varepsilon_{p2}/\varepsilon_{p1}) \quad (22)$$

A similar law has been used in order to explain the primary micro creep strain $\varepsilon \sim \exp[(t/t_0)^{1/3}]$ observed in polymers under ageing [4, 13].

Finally the non-elastic strain writes from Equations 3 and 8:

$$\varepsilon_p = N\varepsilon_{p_0} = (BK)^{-1} = \sigma_B/K \quad (23)$$

so that the non-elastic strain-rate can be expressed from Equation 10 in terms of the constant $\sigma_B$ and the work-hardening rate $K$, as:

$$\dot{\varepsilon}_p = (\sigma_B/K)\nu_N \exp -(\Delta G_a(\sigma - \sigma_i)/kT) \quad (24)$$

instead of Equation 13, for the early preyield stage of a compressive test at a constant total strain-rate. This last equation shows that $K$-measurements are merely a characterization of the pre-exponential term in the

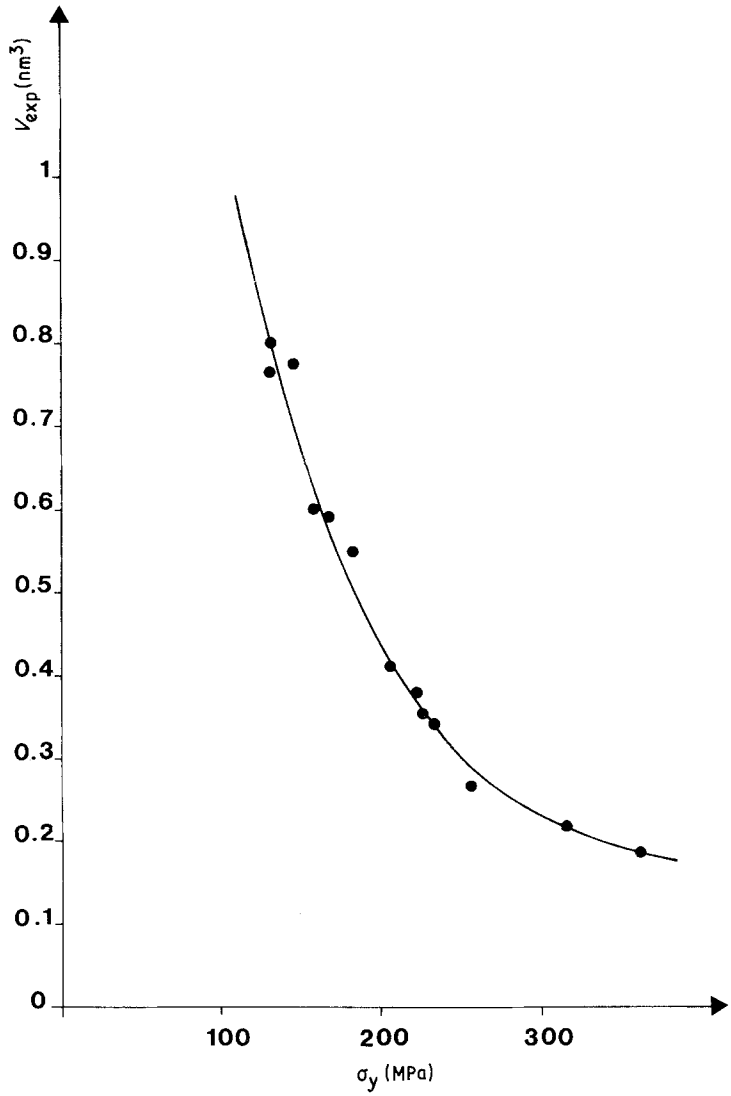


*Figure 6* The experimental activation volume $V_{exp}$ measured at yield versus the yield stress $\sigma_y$.

Arrhenius relationship, fitted to tracking the nucleation processes and therefore sensitive to the resin microstructure at a mesoscale, that is at a scale of typically 1 $\mu$m. In contrast, $\Delta G_a(\sigma - \sigma_i)$ in the argument of the exponential controls the yield stress versus temperature curve (which is obtained in inverting Equation 10, $\Delta G_a(\sigma - \sigma_i) = kT \log [N(\varepsilon_{p_0})_{yield} \nu_N \dot{\varepsilon}_p^{-1}]$ taking $\dot{\varepsilon}_p$ as constant at yielding; it depends therefore mainly on obstacles to defect propagation, i.e. on the chain flexibility and on the entanglement spacing [13]; that is on the resin microstructure to a finer scale, typically 10 nm. It follows that $K$ measurements are not sensitive to the same structural ingredients as the yield stress, and provide a complementary structural probe.

Creep studies can alternatively be used in order to investigate the nucleation of shear defects. In particular, creep in the lower temperature range and below the yield stress gives a direct way of checking if there is any thermal activation in the number of created defects since the behaviour of the defect stock stored in loading the polymer is followed later on through the creep strain under conditions where recovery processes should not take place. Recent experiments in the laboratory show the creep strain increases with time as log $(t + c)$, i.e. proceeds only by exhausting the initial defect stock without any thermal renewing [4], thereby giving evidence that no thermal activation occurs under these conditions. A further report on these experiments will appear soon [16].

## Acknowledgements

The authors wish to thank Rhône Poulenc Industries (Centre de Saint-Fons) for providing PABM resins and to acknowledge the Ministère de la Recherche et de la Technologie for its financial help under contract no 83-P-0493.

## References

1. C. BULTEL, J. M. LEFEBVRE and B. ESCAIG, *Polymer* **24** (1983) 476.
2. J. M. LEFEBVRE, C. BULTEL and B. ESCAIG, *J. Mater. Sci.* **19** (1984) 2415.
3. G. COULON, J. M. LEFEBVRE and B. ESCAIG, *Polym. Bull.* **12** (1984) 339.
4. B. ESCAIG, in "Plastic Deformation of Amorphous and Semi-Crystalline Materials", Edited by B. Escaig and C. G'Sell (les Editions de Physique Publications, Les Ulis, 1982) p. 187.
5. J. M. LEFEBVRE, B. ESCAIG and C. PICOT, *Polymer* **23** (1982) 1751.
6. P. B. BOWDEN, in "The Physics of Glassy Polymers", Edited by R. N. Haward (Applied Science Publishers, London, 1973) p. 279.
7. B. ESCAIG, in "Dislocations in Solids", Yamada Conference, Edited by H. Suzuki *et al.* (University of Tokyo Press, 1985) p. 559.
8. C. BULTEL, Thèse de 3ème cycle (1982).

9. J. M. LEFEBVRE, G. COULON and B. ESCAIG, to be published.
10. J. M. LEFEBVRE, B. ESCAIG, G. COULON and C. PICOT, *Polymer* **26** (1985) 1807.
11. G. COULON, M. RAWISO, J. M. LEFEBVRE, B. ESCAIG and C. PICOT (submitted for publication).
12. U. F. KOCKS, A. S. ARGON and M. F. ASHBY, *Progr. in Mat. Sci.* **19** (1975) 110.
13. B. ESCAIG, *Polym. Eng. Sci.* **24** (1984) 737.
14. M. CAGNON, "Dislocations et Déformation Plastique" (Per Edition de Physique, Paris, 1979).
15. L. P. KUBIN, *Phil. Mag.* **30** (1974) 705.
16. X. CAUX, G. COULON and B. ESCAIG, *Polymer* in press.

*Received 11 March*
*and accepted 14 August 1985*